Inclusive production of X$\to b\bar{b}$ plus a recoil for the LHC Run-II

Nicolas Gutierrez[1,2]

[1] *Department of Physics and Astronomy, University College London - London, WC1E 6BT, United Kingdom*
[2] *Institute for Particle Physics Phenomenology, Department of Physics, Durham University - DH1 3LE, United Kingdom*

arXiv:1604.01438v1 [hep-ph] 5 Apr 2016

PACS aa/bb/cc – First pacs description
PACS aa/bb/cc – Second pacs description

Abstract – This letter presents a study of the inclusive production of X$\to b\bar{b}$ plus a recoil, using simulated samples of pp collisions at $\sqrt{s} = 14$ TeV for an integrated luminosity in the range between 30 fb^{-1} to 3 ab^{-1}. The case for experiments to include un-prescaled b-tag multijet triggers for this topology is made and the ideal jet thresholds are discussed. The sensitivity to Standard Model Higgs with a transverse momentum of at least 200 GeV is evaluated with respect to a continuous background, dominated by multijet processes. The mass of b-jet-pairs is analysed, quoting sensitivity to cross-sections in the range of 1 to 2 pb, for 100 fb^{-1}, covering the Higgs production cross section of 1.8 pb. The trigger strategy presented in this letter is compared to triggers already in use, showing an increase on the signal efficiency for masses below 200 GeV and a performance comparable to a logic OR of all the currently available akin triggers for higher masses. The robustness of the expected sensitivity against systematic uncertainties is estimated by considering various typical sources, such as those on the fitting parameters of the continuous background, shape uncertainties affecting the signal acceptance and the background modelling. The accuracy of a Higgs production cross section measurements is also discussed, quoting sensitivity to deviations of 50% for 100 fb^{-1} and 10% for 3 ab^{-1}.

Introduction. – Although the Higgs boson has been discovered at the LHC [1,2], a 5σ observation for its largest decay mode $H \to b\bar{b}$ has not been achieved so far. The combination of huge backgrounds with large modelling uncertainties transform the observation of this hadronic decay mode in a non-trivial task. The usual production channels, Higgs-Strahlung (VH), associated top-pair Higgs $t\bar{t}H$ and Vector Boson Fusion (VBF), provide upper limits on the event rate of respectively 1.4, 1.5 and 2.8 times the Standard Model (SM) expectation [3–5]. Measuring the Higgs-bottom coupling is of crucial importance at the LHC. Not many channels to measure this coupling exist. So far only HZ, ttH and VBF have been studied [6–10]. In this letter, a new channel in gluon fusion is explored.

The early observation of $H \to \gamma\gamma$ at the LHC demonstrates that despite a small signal to background ratio, a data-driven background approach, high statistics and control over systematic uncertainties can yield a discovery. This letter explores the possibility of pursuing this strategy for the SM $H \to b\bar{b}$ channel, as well as for the search for SM Z-bosons and Beyond the SM CP-odd (A) bosons decaying into $b\bar{b}$ predicted by the two-Higgs-doublet model (2HDM).

The study presented here explores the boosted $X \to b\bar{b}$ kinematic regime such that the combinatorics are reduced, yet each heavy resonance X decay can still be resolved via standard jet-clustering algorithms with typical jet-radius. Requiring high-p_{T} jets is further motivated by the limited capability of trigger systems of detectors to record events with a high rate. This, however, can be compensated by triggering on events with multiple b-jets, which is the strategy explored in the following. The dominant multi-jet background comes from the pure QCD $b\bar{b}$+jets production. Additional b-jets from $g \to b\bar{b}$ may be present in both signal and background - all such candidates are included in the analysis. Interestingly, the $Z \to b\bar{b}$ channel has already been measured using the 8 TeV data with a similar analysis strategy [11].

This letter is organised as follows: First, the analysis strategy is presented, devoting special emphasis to the background fitting approach. Second, the LHC Run II bounds to the SM Higgs and Z bosons via the strategy proposed here are derived.

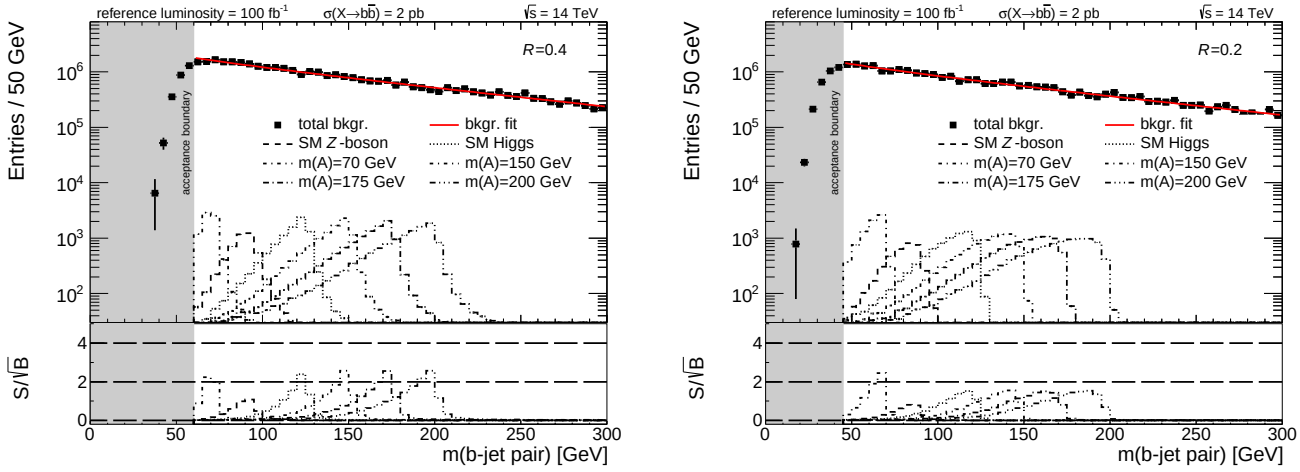

(a) $R = 0.4$ (b) $R = 0.2$

Fig. 1: Invariant $b\bar{b}$ mass distribution for the signal hypothesis and total background contribution. Signal samples with masses between 70 and 200 GeV are shown. The total background is fitted to the dijet mass shape shown as the continuous line (red). The bottom panel displays the ratio between the signal yield and the expected statistical uncertainty on the background. A cross-section of 2 pb for all the signal samples is used.

Event Generation and Analysis. – Signal Monte Carlo (MC) samples are generated for scalar and pseudo-scalar production with MCFM+PYTHIA8 [12, 13] accounting for the full top and bottom mass effects in the production vertex. The higher order QCD effects are included with a flat correction factor of $K \sim 1.6$ [14,15]. For the Z-boson signal and dijets and $t\bar{t}$+jets backgrounds, the SHERPA event generator in the four-flavour scheme [16] is used. All spin correlation effects in the Z and top decays are accounted for. These samples are merged up to two extra jets via the CKKW algorithm [17, 18].

The simulated events are analysed using RIVET [19], which makes extensive use of FASTJET [20, 21] for the jet finding. Jets are defined with the anti-k_t algorithm with a radius $R = 0.4$ satisfying $p_{\mathrm{T}} > 30$ GeV and $|\eta| < 3.0$. To be able to reconstruct the resonance $X \to b\bar{b}$ and suppress the combinatoric background, two b-tagged jets are required. A b-tagging efficiency of 70% and 1% of mis-tagging rate [22] are assumed.

Any event with an isolated electron or muon is rejected. A lepton is isolated if the hadronic transverse energy within a cone of $R = 0.2$ surrounding the lepton tantamount to less than 20% of the lepton transverse energy deposited. Boson-candidates are reconstructed by adding the four-vectors of the two b-tagged jets. Each candidate is required to have a minimum transverse momentum of $p_{\mathrm{T}} > 200$ GeV.

Fig. 1a shows the invariant mass distribution for the Higgs, Z and pseudo-scalar A signals and total background after the event selection. The background is fitted to a functional form

$$p_1(1-x)^{p_2}x^{p_3}. \qquad (1)$$

An equivalent function is used in similar searches for resonances against a steeply falling background in hadronic final states [23, 24]. Also in this Fig., all the signal cross-sections are set to 2 pb. A reference luminosity of 100 fb^{-1} is used. The bottom panel illustrates the expected sensitivity, by computing a bin-by-bin ratio of the number of expected signal events to the statistical uncertainty on the background prediction. The grey shaded area illustrates the lower bound of the fitting range. This boundary is caused by the $R = 0.4$ jets no longer being able to resolve each b-hadron as an individual jet. This can be illustrated by running the event selection with a smaller jet-radius

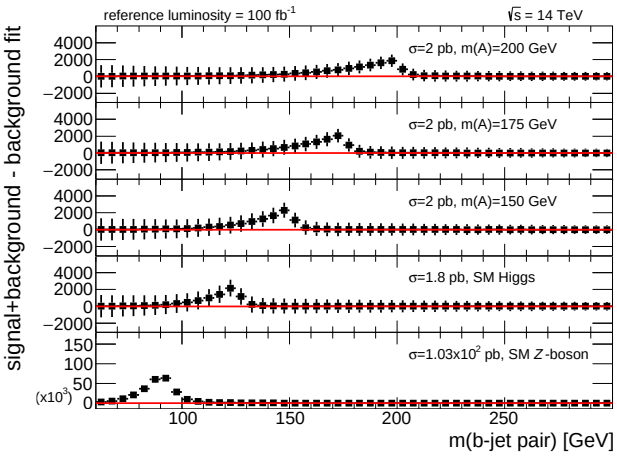

Fig. 2: Difference between the signal-injected background and the background fit for the SM Higgs and Z bosons, Higgs and the pseudo scalar boson $m_A = 150,\ 175,\ 200$ GeV signal samples. The signal injection is performed and shown for each signal sample separately.

parameter $R = 0.2$, see Fig. 1b. Here, the reach of the fitted form for low masses increases by 15 GeV. The usage of a smaller R-parameter, however, also increases the out-of-cone radiation, therefore degrading the signal mass resolution. Techniques to better resolve the collimated $b\bar{b}$ system usually rely on jet-substructure technics [25–27]. However, this is outside of the scope of this paper as most of the signal events are in the resolved regime for our considered mass points.

Fig. 2 shows the difference between signal-injected background and the background fit using the generator cross-section predictions for the SM Higgs and Z bosons, and a fixed 2 pb cross-section for CP-odd bosons for a reference luminosity of 100 fb^{-1}. This illustrates the size of the expected signal bump with respect to the statistical uncertainty on the background prediction.

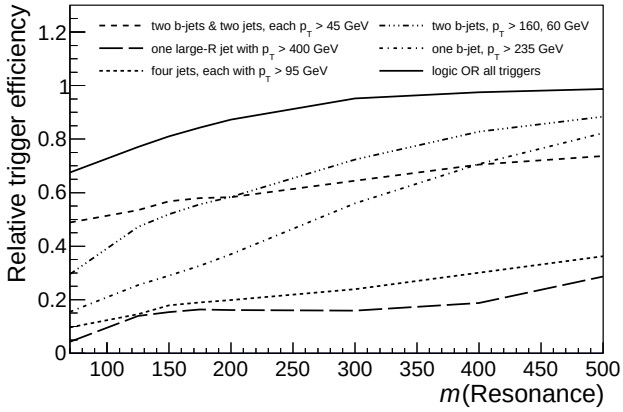
two b-jets & two jets, each p_T > 45 GeV
one large-R jet with p_T > 400 GeV
four jets, each with p_T > 95 GeV
two b-jets, p_T > 160, 60 GeV
one b-jet, p_T > 235 GeV
logic OR all triggers
Relative trigger efficiency
m(Resonance)

Fig. 3: Efficiency of various triggers and for the combination of all these triggers.

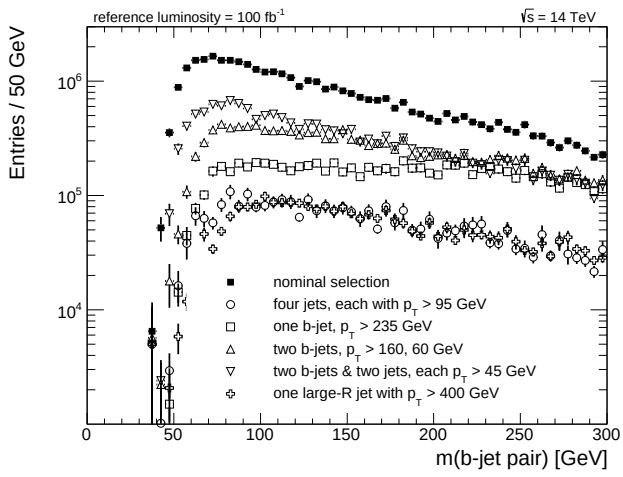
reference luminosity = 100 fb^-1
√s = 14 TeV
Entries / 50 GeV
nominal selection
four jets, each with p_T > 95 GeV
one b-jet, p_T > 235 GeV
two b-jets, p_T > 160, 60 GeV
two b-jets & two jets, each p_T > 45 GeV
one large-R jet with p_T > 400 GeV
m(b-jet pair) [GeV]

Fig. 4: Total background shape for various triggers. For each, the acceptance boundary is given by the point at which the distribution has reach its maximum and it can no longer be described as a steeply falling background.

Trigger effects. It is natural to expect that for a very large integrated luminosity the $H \to b\bar{b}$ process would eventually become significant over the statistical uncertainty of a continuous background. This strategy, however, has not been pursued by experimental collaborations in part due to the limited rate of triggered events that can be recorded. Fig. 3 shows the efficiency of the most akin triggers currently included in active trigger menus. Individually, none of these triggers goes above a 50% efficiency, for the SM Higgs. This efficiency increases for larger masses. When combining events collected via all trigger strategies, an 80% of efficiency for the SM Higgs and nearly a 100% for very large masses is achieved. Notice that each trigger yields a different background shape and acceptance boundary. In the combination of all triggers, the acceptance boundary is still shifted to 80 GeV therefore limiting the accessibility to $Z \to b\bar{b}$ channel. This is shown in Fig. 4.

In this letter, a trigger with two b-tagged jets recoiling against one or more jets is proposed, requiring in addition the p_{T} of a b-tagged jet pair to be above 200 GeV.

Results. – The boson-candidates mass distribution is analysed in a maximum-likelihood fit using HistFitter [28]. Fig. 5 shows the expected 95% CL limit on the cross-section times branching ratio of a Higgs or Z bosons decaying into $b\bar{b}$, $\mathcal{BR}(X \to b\bar{b})$. For Z bosons, with only 1 fb^{-1}, sensitivity to cross-sections around 20 pb is observed. For the SM Higgs and 100 fb^{-1}, two-sigma sensitivity to a cross-section of around 2 pb is observed. This is in agreement with the simple $\mathrm{S}/\sqrt{\mathrm{B}}$ shown in Fig. 1a. Notice that the early Z-boson observation becomes ideal for an *in-situ* uncertainty constraint to be used in the later $H \to b\bar{b}$ measurement.

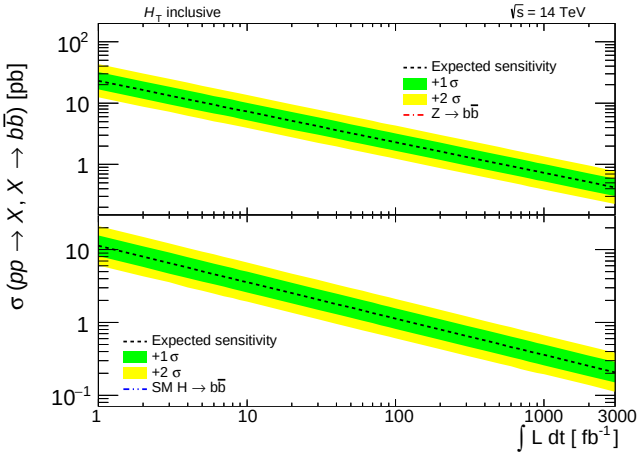

Fig. 5: Expected sensitivity to SM Z-boson (top panel) and Higgs (bottom panel) inclusive production in the X+jets topology. This is presented against the integrated luminosity. For comparison, the SM cross-section prediction for these processes is also shown.

Robustness against systematic uncertainties. The impact of various potential sources of systematic uncertainties is studied by varying the signal and background rates and shapes. The aim is to access the impact of potential extra sources of uncertainties that were not accounted so for in the MC generation, as for instance, detector effects. In HistFitter, each systematic variation is associated to a nuisance parameter that is fitted simultaneously with the signal strength. Nuisance parameters can be constrained by the data, corresponding in this case to the MC background prediction. Large uncertainties, as those testing the background MC modelling, are over-constrained minimising their impact. This undesired feature can be avoided by separating uncertainties in two classes: those likely to be encountered in a real data-driven background scenario and those that are only relevant when considering the potentially inaccurate description of the background by the MC. The former are assigned nuisance parameters while to test the impact of the latter the nominal background prediction is substituted by the systematic variation.

Fig. 6 compares the nominal sensitivity to that obtained after including a given uncertainty, for an integrated luminosity of 100 fb^{-1}. The top entry shows the nominal value. The error bars correspond to $\pm 2\sigma$. The central panel shows the impact of uncertainties considered as nuisance parameters, such as those affecting the signal acceptance and the statistical uncertainty on the parameters of Eq. 1. From this class, the uncertainty on the signal mass resolution is shown to have the largest effect, particularly on the $\pm 2\sigma$ band. The bottom panel shows the impact of uncertainties due to the MC modelling of the background. Apart from a 50% drop on the MC background cross-section, which as expected improves the sensitivity, these uncertainties have a minor impact on the overall result.

SM Higgs production cross-section measurement. The sensitivity to deviations from the SM Higgs production cross-section prediction is tested by assuming the signal hypothesis

$$N_{\text{obs}} = N_{\text{SM H}\to\text{b}\bar{\text{b}}} + N_{\text{signal}}, \qquad (2)$$

where N_{signal} is proportional to the fitted parameter σ'. Here N_{obs} is given by the number of expected events from multi-jet, $t\bar{t}$ and SM H$\to b\bar{b}$. Fig. 7 shows the expected sensitivity relative to the SM prediction. Here, for an integrated luminosity of 100 fb^{-1}, a sensitivity to 50% deviations is achieved. At the high luminosity LHC $\mathcal{L} =$ 3 ab^{-1} a sensitivity of 10% deviations can be obtained.

Summary. – This is the first study to demonstrate a simple and feasible strategy for discovering $X \to b\bar{b}$ exploring the continuous and steeply falling background via a suitable fit. In this letter is shown that the 14 TeV LHC can observe the $X \to b\bar{b}$ decay very early for the Z and Higgs bosons. Moreover, the Higgs uncertainties for this decay can achieve 10% for the high luminosity LHC, therefore competitive to the other production channels.

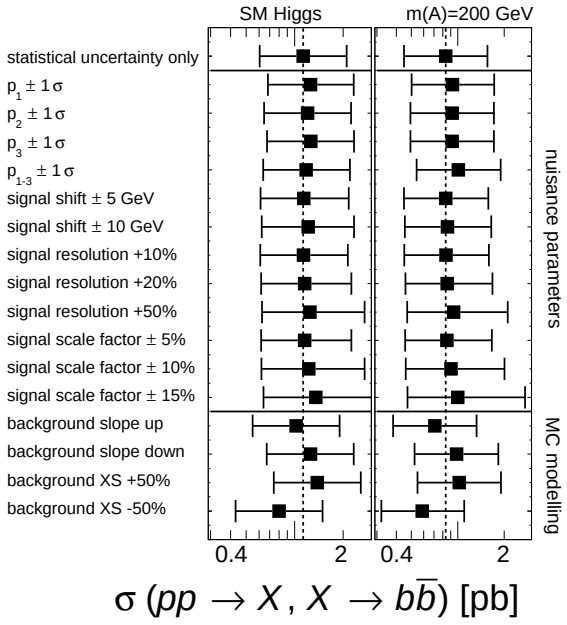

Fig. 6: Comparison between the expected sensitivity to the signal cross-section times $\mathcal{BR}(X \to b\bar{b})$ for the statistical uncertainty only and the limit after the addition of individual sources of uncertainties. This is shown for SM Higgs (left) and pseudo-scalar $m_A = 200$ GeV (right) hypotheses. The marker shows the central value while the error bar corresponds to a $\pm 2\sigma$ band.

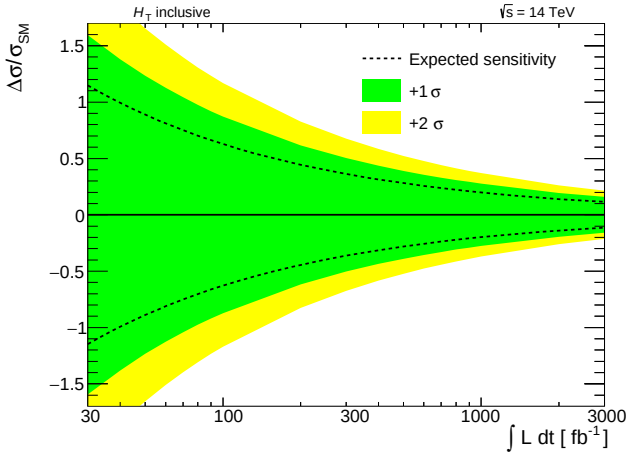

Fig. 7: Expected sensitivity to deviations from the SM $H \to b\bar{b}$ cross-section prediction.

* * *

NG thanks Jon Butterworth, James Ferrando, Andy Pilkington and Michael Spannowsky for useful discussions. Also, thanks to Dorival Gonçalves for helping with the generation of the signal samples. This work is supported

Table 1: Signal and background acceptance measures, presented inclusively and in bins of H_{T}, corresponding to the following ranges in GeV: 400-600; 600-1000; 1000-1600; 1600-2500; 2500 and beyond. For background, the measure shown is the cross-section corresponding to the fraction of events after event selection, including tagging and mistagging efficiencies. This is followed, after the comma, by the lower boundary of the m(b-jet pair) spectrum that can be be described by the function used. The symbol – is used for bins where either the functional form does not describe the background or the MC statistics are insufficient. For signal, the selection efficiency is shown comma-separated to the fraction of selected events within a 10% mass window around the generator mass for each sample.

inclusive	H_{T} bin 1	H_{T} bin 2	H_{T} bin 3	H_{T} bin 4	H_{T} bin 5
Total background cross-section times selection acceptance [pb], acceptance boundary [GeV]					
4.9e+02, 60	2.8e+02, 60	1.6e+02, 90	22, 100	2.8, –	0.21, –
Signal signal selection efficiency, fraction of selected events within 10% mass window					
SM Z-boson					
0.055, 0.72	0.036, 0.72	0.015, 0.7	0.0008, 0.58	3.5e-05, 0.38	9.9e-07, 1.4e-08
SM Higgs-boson					
0.1, 0.69	0.052, 0.7	0.04, 0.68	0.0064, 0.72	0.00099, 0.6	0.00036, 0.17
m(A)=70 GeV					
0.092, 0.83	0.056, 0.85	0.028, 0.8	0.0018, 0.52	0.00028, 0.073	0.00029, 0.0072
m(A)=200 GeV					
0.14, 0.53	0.057, 0.54	0.065, 0.52	0.012, 0.56	0.0029, 0.66	0.00091, 0.54

by the 7th Framework Programme of the European Commission through the Initial Training Network HiggsTools PITN-GA-2012-316704.

REFERENCES

[1] Aad G. *et al.*, *Phys.Lett.B*, **716** (2012) 1.
[2] Chatrchyan S. *et al.*, *Phys.Lett.B*, **716** (2012) 30.
[3] Chatrchyan S. *et al.*, *Phys.Rev.D*, **89** (2014) 012003.
[4] Aad G. *et al.*, *Eur. Phys. J.C*, **75** (2015) 349.
[5] Khachatryan V. *et al.*, *Phys. Rev.D*, **92** (2015) 032008.
[6] Butterworth J. M., Ochoa I. and Scanlon T., *Eur. Phys. J.C*, **75** (2015) 366.
[7] Soper D. E. and Spannowsky M., *JHEP*, **08** (2010) 029.
[8] Englert C., Mattelaer O. and Spannowsky M., , (2015) .
[9] Moretti N., Petrov P., Pozzorini S. and Spannowsky M., *Phys. Rev.D*, **93** (2016) 014019.
[10] Plehn T., Salam G. P. and Spannowsky M., *Phys. Rev. Lett.*, **104** (2010) 111801.
[11] Aad G. *et al.*, *Phys. Lett.B*, **738** (2014) 25.
[12] Campbell J. M. and Ellis R., *Nucl.Phys.Proc.Suppl.*, **205-206** (2010) 10.
[13] Sjostrand T., Mrenna S. and Skands P. Z., *Comput. Phys. Commun.*, **178** (2008) 852.
[14] Campbell J. M., Ellis R. K., Frederix R., Nason P., Oleari C. and Williams C., *JHEP*, **07** (2012) 092.
[15] Buschmann M., Englert C., Goncalves D., Plehn T. and Spannowsky M., *Phys. Rev.D*, **90** (2014) 013010.
[16] Gleisberg T., Hoeche S., Krauss F., Schoenherr M., Schumann S., Siegert F. and Winter J., *JHEP*, **0902** (2009) 007.
[17] Catani S., Krauss F., Kuhn R. and Webber B. R., *JHEP*, **11** (2001) 063.
[18] Hoeche S., Krauss F., Schumann S. and Siegert F., *JHEP*, **05** (2009) 053.
[19] Buckley A., Butterworth J., Lonnblad L., Grellscheid D., Hoeth H. *et al.*, *Comput.Phys.Commun.*, **184** (2013) 2803.
[20] Cacciari M., Salam G. P. and Soyez G., *Journal of High Energy Physics*, **2008** (2008) 063.
[21] Cacciari M., Salam G. P. and Soyez G., *Eur.Phys.J.C*, **72** (2012) 1896.
[22] Aad G. *et al.*, , (2015) .
[23] ATLAS Collaboration, , (2015) .
[24] CMS Collaboration, , (2015) .
[25] Butterworth J. M., Davison A. R., Rubin M. and Salam G. P., *Phys. Rev. Lett.*, **100** (2008) 242001.
[26] Krohn D., Thaler J. and Wang L.-T., *JHEP*, **06** (2009) 059.
[27] Thaler J. and Wilkason T. F., , (2015) .
[28] Baak M., Besjes G. J., Cte D., Koutsman A., Lorenz J. and Short D., *Eur. Phys. J.C*, **75** (2015) 153.

Boosting the $b\bar{b}$ system. – To further decrease the event rate, the jet p_{T} threshold could be raised, therefore boosting the $b\bar{b}$ system. The system boost is parametrised in terms of the scalar sum of all jets passing the event selection H_{T}. The global observable H_{T} is chosen instead of the more intuitive $b\bar{b}$ pair p_{T}, as it does not require to uniquely identify a candidate, in line with the inclusive approach presented in this paper.

Table 1 summarises the changes on the signal and background acceptance in terms of the overall boost of system. Here, the total background cross-section drops by one (two) orders of magnitude for the 3^{rd} (4^{th}) H_{T} bin, regardless of R. This drop is accompanied by a reduction of the fitting range and of the signal efficiency for SM Z-bosons and hence, from the 2^{nd} H_{T} bin onward, sensitivity to this process is not expected. For the lowest mass points, $m_A = 70$ GeV and to a lesser extent for SM Z-bosons, at very-large H_{T}, a considerable loss in sig-

nal acceptance and mass resolution is observed. This loss could be recovered by using $R = 0.2$, however, this change is observed to bring little improvement to the other mass points, in all but the final H_{T} bin, showing that the bulk of the events is in the resolved regime, except for very low mass signals at very-large H_{T}.